CONTAINMENT OF EXPLOSIVE BLAST IN A SPHERICAL VESSEL WITH NOZZLES

L Lazari*, S J Burley and S T S Al-Hassani
University of Manchester Institute of Science and Technology, PO Box No. 88, Manchester M60 1QD, UK.
*Currently at the High Technical Institute, Aglanjia, Nicosia, Cyprus

The problem of using explosives inside a closed spherical pressure vessel of 1.83m (72") diameter with nozzle attachments is considered. Theoretical and experimental analyses of the response are used to examine the safe use of the vessel as an explosive chamber. Prior to conversion the vessel underwent extensive static analysis, both experimental and theoretical.

Explosive charges up to 150 g were detonated within the chamber and the blast pressure and shell response measured by transducers. A finite element analysis was performed and found to agree well with the experimental data including areas where the classical analysis was in disagreement. The procedure for determining the safe explosive mass is outlined.

INTRODUCTION

Operations such as explosive welding, forming, compaction, etc., involving small explosive charges, up to 10 g, can be carried out using ear defenders and a minimum of blast protection. If, however, large scale operations involving a few kilograms of explosive are to be carried out the choice of a site to accommodate such operations becomes a problem.

In the course of explosive welding research a simple, safe explosive chamber had to be designed. The main requirement was that it should safely contain repeated firing of explosive charges up to a few hundred grams. The chamber would be sited inside a laboratory about 20m away from offices. It was obviously important that explosions in this chamber should not cause damage to the building fabric nor should they create excessive noise. Other features to be incorporated were the need for ease of positioning of charge and the extraction of explosion fumes before entry of personnel for recovering of the workpiece. Later on the requirement of the chamber was increased to accommodate work on explosive cutting of small scale structures. This has initiated the present study.

BACKGROUND

In several fields of engineering and science, there are requirements for safe gastight or near gastight structures which must withstand the effects of internally applied dynamic loads. Examples of such structures include:

(a) Blast chambers, within which the effects of explosives or propellants can be studied under controlled atmospheric conditions

(b) Safety chambers, for proof testing of small pressure vessels

(c) Nuclear-reactor containment structures designed to contain the effects of accidental runaway from the reactors which they house.

Depending on the engineering application, these structures may have to withstand static as well

as dynamic pressures, therefore, they are usually constructed in the form of large-sized, thin-walled pressure vessels, such as spherical or cylindrical shells with hemispherical or ellipsoidal end caps.

In designing such structures, it is necessary to consider their dynamic response to the expected transient pressure and to determine whether the static pressure design criteria are sufficient. The simplest analytical problem relating to the design of these structures is that of the response of a spherical shell to a spherically symmetric transient pressure on its inner surface. Baker and Allen (1) considered the elastic response of a spherical shell of any thickness to such a pressure pulse. They showed that the response of even relatively thick shells could be adequately described by an approximate "thin-shell" equation of motion. Baker (2) extended the analysis to include plastic deformation and the nonlinear effects of shell thinning and increase in radius, and obtained solutions to these problems.

The same equation for the dynamic pressure, resulting from an explosion in a spherical chamber filled with air used by Baker et al (1) was later adopted by Zhdan (3), together with a system of equations of one-dimensional gas dynamics in an attempt to determine the dynamic load and the impulse acting on the wall of the chamber. In order to do so, the effect of pressure macropulsation at the wall and the possibility of resonance of the chamber was examined. From experiments, it was concluded that resonance of the chamber will occur when the displacement of the chamber shell relative to the equilibrium position is larger than the displacement in the quarter of the first period of intrinsic oscillation, predicted by equation (1), see ref. (3) for details.

$$\delta_{max} = J_{ref}/\rho_w \, h\omega \qquad\qquad\qquad (1)$$

where, δ_{max} is the maximum shell displacement, J_{ref} is impulse per unit area, h is the shell thickness and ω is the frequency of vibration.

This effect must be taken into account in designing the chamber for maximum explosive charge weight. Quantitative analysis of the results obtained by Zhdan (3) shows that at resonance of the first pressure macropulsation, the additional impulse acting on the spherical shell in the course of its radial expansion may be as much as 50% of the original impulse.

Similar observations were made by Buzukov (4,5) who used the same approach to study the effect of internal blast loading of a cylindrical chamber. In examining the experimental strain amplitude results, it was noticed that the peak deformation of the chamber was higher in later cycles than that of the first oscillation. Approximately 20-40 μsec after the start of movement, the walls of the chamber were "set swinging". The excess of the maximum deformation over the initial deformation reached 100-150% in the case of relatively small charges and was reduced to 30-40% for larger explosions. This is in close agreement with Zhdan's (3) findings of a 50% increase in the original impulse acting at the wall of a spherical shell at resonance.

The "swinging" observed by Buzukov (4,5) was found to originate 20-40 μsec after arrival of the shock wave at the side walls of the chamber. This appearance cannot be explained by the secondary shock of the reflected wave, since the transit time of the reflected wave in this chamber design was 3-5 msec. It is obvious that the phenomenon is associated with a complex oscillatory process of the whole structure and, in particular, with the fact that the natural frequencies of the radial and longitudinal oscillations of the wall are close. The same phenomenon was observed by Zhdan et al (3,6) and Adischev et al (7,8) who attributed the increase in the magnitude of spherical and cylindrical shell displacements to the possibility of a resonance effect of the chambers in question.

Ivanov et al (9) used destructive tests and statistical theory to evaluate the fracture strength of explosion chambers. The specimens were made of steel of ellipsoidal shape and variable wall thickness. The vessel models were filled with water and they were internally blast loaded to failure to check for a scale effect on the fracture strength of explosion chambers. They found

that there is a marked scale effect in explosive loading of similarly loaded geometrically similar pressure vessels filled with water. They concluded that this scale effect is of energy character and is in accordance with the findings of references (10-12).

An entirely different approach was employed by Ahrens et al (13) in an attempt to obtain an expression for the peak pressure generated by the expansion of detonation products in evacuated chambers. Using small charges (0.2 to 2 g) of HNS (Hexanitrostilbene) explosive in vacuums of 10^{-4} to 5×10^{-6} kPa they found that the resultant gas blast rapidly achieves a terminal velocity of 1.0 to 1.2 km/sec. From their experimental measurements they suggested that the reflected peak pressure may be represented by

$$P = 6.5 \times 10^5 \ r^{-3.5} \ (bar) \tag{2}$$

where r is the ratio of the radius from the centre of the charge to the transducer to the radius of an equivalent charge. Similar results for the exponent of r were obtained by Lutzky (14) for the fall off of the gas blast at a distance of 10 charge radii from a 1-1b PETN sphere detonated in vacuum.

The pressures generated by an explosion in evacuated chambers was also studied by Dawson et al (15) who carried out systematic explosive tests in a cylindrical mild steel bell in order to obtain data for the design of an explosion chamber for high energy rate forming purposes. The chamber was evacuated to a pressure of less than 3 kPa and explosive charges (of Trimonite 1) of up to 550 g were detonated.

For charges up to and including 130 g the pressure in the vessel the quasi-static final overpressure was found to be approximately given by,

$$P = \frac{0.145 \ W}{V} \tag{3}$$

where p is in kPa, W explosive charge input in gm and V the volume of the vessel in m^3.

ANALYSIS

The chamber under consideration is a spherical steel pressure vessel of 1.83 m (72") outside diameter and 25.4mm (1") wall thickness. Three pad reinforced nozzles of diameters 0.22mm, 0.41m and 0.61m were attached (See Fig.1). The steel used was BS1501-161 26A. Gill (16) performed tensile tests on a selection of materials and found values of 200GPa for the Young's modulus, 0.275 for the Poisson's ratio, and 300 MPa for the lower yield stress. The vessel had been studied over several years and the design pressures, stresses and limitations were well known, see Gill (16), Paine (17) and Kannas (18).

The present paper highlights the analytical and experimental steps taken in deciding the safe limit of this vessel for explosive working.

Thin Shell Formulation of the Problem

A closed-form thick shell, arbitrary loading solution would be extremely difficult to generate and unwieldy to use. By making some engineering assumptions a usable equation has been formed by Baker et al (1) for spheres. The major assumptions are:-

(i)   only radial motion is considered
(ii)   thin shell theory is applied
(iii)   the internal pressure loading is of the form $P = P_p(1-t/T)$

Consider the shell element shown in Fig. 2, subjected to an internal transient pressure $P(t)$. From thin shell theory it may be assumed that the radial strain ϵ_r and the radial stress σ_r are negligible in comparison with tangential strains and stresses, and that the variation of the tangential strains and stresses through the thickness of the shell is small. Then the equation of motion in the radial direction of the shell element shown in Fig. 2 is,

$$h \ (\sigma_\theta + \sigma_\phi) + \rho h b \ \frac{d^2 u_r}{dt^2} = bP(t) \tag{4}$$

Using Hooke's law and since, $\epsilon_\theta = \epsilon_\phi = \dfrac{u_r}{b}$, equation (4) becomes

$$\rho \ \frac{d^2 u_r}{dt^2} + \frac{2E}{1-\upsilon} - \frac{u_r}{b^2} = \frac{1}{h} \ P(t) \tag{5}$$

The solution of this equation, for the blast pulse

$$\left. \begin{aligned} P(t) &= P_p\left[1 - \frac{t}{T}\right], \quad 0 < t \le T \\[6pt] P(t) &= 0 \qquad\qquad\qquad t > T \end{aligned} \right] \tag{6}$$

is, see Baker et al (1)

$$\left. \begin{aligned} u_r &= K \left[1 - \frac{t}{T} - \cos \omega t + \frac{\sin \omega t}{\omega T}\right] \quad 0 < t \le T \\[6pt] u_r &= A \cos \omega(t-T) + B \sin \omega(t-T) \qquad t > T \end{aligned} \right] \tag{7}$$

where

$$\omega^2 = \frac{2E}{\rho b^2 (1-\upsilon)} \ , \quad K = \frac{P}{\omega^2 \rho h} \tag{8}$$

and

$$\left. \begin{aligned} A &= K \left[\frac{\sin \omega T}{\omega T} - \cos \omega T \right] \\[6pt] B &= K \left[\sin \omega T + \frac{\cos \omega T}{\omega T} - \frac{1}{\omega T} \right] \end{aligned} \right] \tag{9}$$

According to this approximate theory, the shell vibrates in a single radial mode with a maximum radial displacement of $u_{max} = (A^2 + B^2)^{\frac{1}{2}}$.

The maximum tangential strains are thus given by $\epsilon_{max} = u_{max}/b$ $\quad$ (10)

EXPERIMENTAL WORK

Charges of Trimonite No. 1 were detonated close to the centre of the chamber. Trimonite No. 1, manufactured by ICI Nobels in the UK, is a mixture of anodised aluminium, TNT and ammonium nitrate, and has a yield of 6280 Jg^{-1} and a detonation velocity of about $2000ms^{-1}$, but the latter is known to vary with geometry and confinement.

Strain gauges were mounted on the outside the spherical surface of the chamber and connected via a suitable amplifier to a storage oscilloscope. Dynamic pressure measurements were made using a piezoelectric pressure gauge (Kistler type 607A SN, 0-250 bar, linearity 0.3%) on a suitable mounting in one of the nozzles close to the outside of the chamber. The transducer was positioned to minimise the effect of reflections from the chamber walls. Strain and pressure were recorded for 15 explosions in the mass range 15-141 g.

Strain gauge records for the 56 g and 106 g shots are shown in Fig. 3. The first maximum in the strain amplitude was taken to correspond to the peak pressure.

Pressure records for the 42 g and 63 g shots are shown in Fig. 4. (The second peak is due to reflection from a structure within the chamber and need not concern us here.)

From these recordings the peak strain, peak pressure and overpressure duration were determined. Using the experimentally found P_p and T the values of the constants K, A and B were calculated to give, using equations 7,8,9 and 10, a semi-theoretical value for the first peak strain ϵ_φ

The values for each parameter are listed in Table 1. It can be seen that the agreement between the experimental and the semi-theoretical values are very good, see Fig. 5.

Determination of the maximum allowable explosive charge mass

If the mean lower yield stress of the vessel's material is 300 MPa then the corresponding strain at the threshold of yielding is $\epsilon_y = \sigma_y/E(1+\upsilon) = 1.25 \times 10^{-3}$. By extrapolating from the P_{max} vs ϵ_θ relationship of Fig. to $\epsilon = 1.25 \times 10^{-3}$ the dynamic pressure required to cause yielding of the material is $P_{yd} \simeq 24$ MPa. From the static analysis of thin spherical pressure vessels the pressure required to cause yielding is given by

$$P_{ys} = \frac{2h\ \sigma_y}{a} \approx 17 \text{ MPa} \qquad (11)$$

where σ_y is the mean lower yield stress.

Thus the dynamic yield pressure is about 30% greater than the static yield pressure. At this point it must be emphasised that the measured dynamic pressure was a 'free field' measurement taken about 300mm away from any structure. The actual dynamic load applied will, of course, be higher due to the reflection of the blast.

Gill et al (16) reported that the design stress of the spherical shell of this veseel is about 140 MPa. Using equation (11) the static design pressure is about 8 MPa and by extrapolating from Fig. 5 for the design strain of 5.6×10^{-4}, the dynamic design pressure will be about 11.4 MPa.

The experimental data for peak pressures obtained from the detonation of various charge weights is listed in Table 1. By plotting peak pressure, P_{max}, against charge weight, W, it was found that an approximate linear relationship could be fitted through the points as shown in Fig. 6. A similar relationship was reported by Dawson et al (15). This result however is not general and only applies to contained explosions of certain geometries.

TABLE 1 - Experimental and theoretical results from the detonation of explosive charges at the centre of the chamber

EXPLOSIVE CHARGE, W, (g)	PEAK PRESSURE P_{max} MPa	CONSTANT $k*10^{-5}$	TIME T μs	ϵ_θ EXPERIM μ-strain	ϵ_θ THEORY μ-strain
15	0.380	2.15	50	6.9	5.7
22	0.428	2.43	60	9.4	8.2
22	0.428	2.43	62	9.6	8.5
27	0.483	2.74	62	12.7	10.9
34	0.518	2.94	90	15.8	15.2
42	0.593	3.36	100	17.4	17.3
52	0.676	3.83	113	24.0	22.5
56	0.704	3.99	116	25.0	23.6
63	0.759	4.30	123	28.5	26.9
78	0.897	5.08	138	36.0	35.3
88	0.952	5.39	144	39.9	38.9
91	0.966	5.47	146	42.2	40.0
106	1.021	5.79	156	46.0	44.9
119	1.104	6.26	164	54.0	50.8
141	1.325	7.51	175	67.0	64.0

If for the sake of argument we assume that the P_{max} vs W relationship of Fig. 6. is valid up to the dynamic design pressure then by extrapolating it was found that the charge required to cause a pressure rise in the chamber of 11.4 MPa is about 1.5 kg. These design pressures and charge weights would also satisfy the design requirements for the pad reinforced nozzles of the vessel since the static analysis (16) indicates that the thickness of the nozzles and that of the welded pads was chosen to fulfil the design pressure requirements. This obviously needs to be substantiated by a dynamic analysis. The explosive charge required to raise the pressure inside the chamber to the dynamic yield pressure of, P_{yd} = 24 MPa, can in this case be estimated from Fig. 6 at W $\simeq$ 3.2 kg ($\simeq$ 7.0 lb).

FINITE ELEMENT MODELLING

The above arguments did not warrant sufficient confidence and a safe limit of 150 g incorporating a generous safety margin was used over many explosions and found to be adequate. The analysis is, however, only strictly applicable to spherical shells, and whilst the strains at the 'equator' of the vessel, well away from the nozzles have been accurately predicted, there was no information on the strains or stresses in the region of the shell/nozzle junctions, where raised stresses would be expected. It was decided to extend the analysis by

the use of finite elements.

The chamber was modelled using a finite element package (ABAQUS) on an Apollo workstation (Model DN4000). Both static and dynamic analyses were performed.

It would be prohibitively expensive in computer time to fully model the chamber using three dimensional elements, so a decision was taken to concentrate on the largest (0.61m outside diameter) nozzle. An advantage of concentrating on this nozzle arises from the fact that this is the main entry/exit route for positioning work within the chamber. The flange is attached by up to 24 (50mm diameter) bolts and the effort required to insert and remove these bolts was such that rarely were more than six used for charges of 50g or so. The analysis should indicate the stress in the bolts and help in deciding safe practice.

To further reduce computer time axisymmetric elements were used. This has the effect of suppressing certain modes of vibration, for example where the cross section of the nozzle deforms into an ellipse.

A further disadvantage was that cross-coupling of the modes of vibration of each nozzle was not allowed for. This manifested itself as an incorrect prediction of the frequency of oscillation, see below. (CPU times were about 700s for a static analysis and about 140000s for the dynamic).

The chamber has been the subject of extensive static analysis and experimental work by Gill (16), Paine (17) Kannas (18) and their data was used to check the model prior to dynamic analysis.

The results of a static analysis are shown alongside experimental data from Paine (17) in Figure 7a and 7b, showing circumferential and meridional stresses for the inside and outside of the branch. The agreement is excellent, and differences between the anlalysis and experiment seem to be mainly due to uncertainties in the position and extent of the welds joining the pad to the nozzle etc. Difficulty was reported by Paine (17) when plotting the experimental data and comparing to classical analysis. The excessive strain at the 'toe' of the weld is due to the sharp inside corner, which is filleted on the chamber. The analysis of the pad gave results closer to those reported by Paine (17). Comparison with classical analysis (17) shows that the finite element method provides more accurate results. It is felt that if the dimensions of the pad, sphere and nozzles, and the extent of the weld was accurately known, the analysis could be improved.

The finite element mesh used is shown in Figures 8 to 10 and consists of 228 two dimensional axisymmetric elements. It was found that a fine mesh was necessary in the sphere/nozzle weld region. As this area contains both the pad/sphere weld and the sphere/nozzle weld this is not surprising.

From the edge view (Fig. 8) it can be seen that the flange plate is a separate entity, coupled to the flange by a pre-stressed truss element. A single interface element separates the flange and the flange plates and represents the seal. Motion in the y-direction (see Fig. 8) was suppressed at the edge of the sphere and motion in the x-direction suppressed at the centre of the flange plate.

Several analyses were performed with the flange plate removed in which the position of the load due to the flange plate was applied at a single point or distributed over the flange. It was found that any variations in the stress distribution were local to the flange and did not propagate far down the nozzle. This was taken to indicate that the modelling of the bolts and seals was not critical.

Analyses were performed with interface elements between the pad and sphere (to stop the structures 'passing through' each other) but it was found that the results were erroneous. This is in agreement with Kitching et al (16) who used an analysis assuming contact at the welds only. The reason is that the movements are small, about 0.6 mm at the design pressure

(8MPa) and the pad is not in intimate contact with the sphere.

Dynamic Loading of the FE model

Loading was via a subroutine in the ABAQUS input deck. The form of the loading is the modified Friedlander equation.

$$P = P_p(1-t/T) \ e^{-\beta t/T}, \tag{12}$$

the simplest form capable of retaining peak pressure, overpressure duration and total impulse. P_p, T and β vary with explosive type, explosive mass and range. Equation (13) can be integrated between t=0 and t=T, to yield the impulse

$$I = \frac{P_p T}{\beta^2} \ (e^{-\beta} -1 + \beta) \tag{13}$$

in terms of P_p, T and β. Baker (19) provides non-dimensional plots of reflected and side on pressure (as P/P_0), reflected and side on impulse as $(Ia_0/P_0^{1/3}E^{1/3})$, overpressure duration as $(Ta_0P_0^{1/3}/E^{1/3})$ and the Mach number for reduced distance $(R \ P_0^{1/3})/E^{1/3}$.

These plots represent summaries of a large number of experiments by many workers of all types of explosive and range.

The loading was split into three regions, the spherical part, the nozzle wall and the flange plate.

The sphere Only explosions at the centre of the chamber were considered, so the shock wave propagates normally to the surface and data on normal reflections were used.

The nozzle It can be shown that a Mach stem must be present along the side of the inside of the nozzle.

The load was determined by calculating the Mach number of the Mach stem as, see (20)

$$M_{stem} = \frac{M_0}{\sin\theta} \tag{14}$$

where θ is the angle between the ray at the shock front/nozzle wall interface and the normal at that point.

Using data in Baker (19) the loading required for this Mach number was calculated and inserted in equation (12) for side loading.

The flange plate Normal reflection from the flange plate was assumed, to avoid having to code in polar reflection curves, and as the deviation from normal is at most about 10^0. This led to excessive loading and thus errs on the side of safety.

Limitations of the loading subroutine Only the initial shock is allowed for. Reflections are assumed to have little effect. The width of the Mach stem is not calculated so the outer region of the flange (by the nozzle) is not loaded correctly. This error is considered to be small.

Results

The results of a dynamic analysis modelling the detonation of 106g of Trimonite at the centre of the chamber is shown in Figs. 11 and 12 and can be compared directly with the strain gauge readings in Fig. 3.

Figure 11 shows strain ϵ_θ (ϵ_{zz} in Figure 9) mid way between the nozzles, on both the inside and the outside of the chamber.

Figure 12 shows strain $\epsilon\varphi$ (ϵ_{yy}) at the same positions. Given that the loading routine uses data for free air blasts, the agreement between the prediction of initial peak strain (about 50 micro strain) and experiment (46 micro strain) is remarkable.

Figure 11 shows that the initial peak does not correspond to the maximum strain reached, as found experimentally and shown in Figure 3.

There is a major quantitative difference between Figures 3 and 11 in that the frequency of oscillation in the strain in Figure 3 is about double that in Figure 11. Figure 12 provides the explanation. After a few milliseconds the strain on the inside and outside of the chamber are 180^0 out of phase, indicating bending at this point. The chamber is not now oscillating as a sphere but rather (looking at Fig. 10) the nozzle and flange plate are oscillating in the y-direction.

Recalling that diametrically opposite to the 0.61m diameter nozzle is a 0.41m diameter nozzle, it is clear that each will oscillate at a slightly different frequency. Furthermore, as each flange plate is at a slightly different distance from the centre of the chamber, the phase of such oscillations will be different. The higher frequencies visible in Figure 3 are due to interference between these modes of oscillation.

The maximum principal stress at the three nodes closest to the 'toe' of the pad/nozzle weld is shown against time in Figure 13. The stress does not exceed 25 MPa and is thus well below the design stress of the vessel (140 MPa).

From this it was concluded that the vessel was entirely safe for 106 g of explosive.

The analysis was repeated for an explosive mass of 1 kg. The principal stresses at the three nodes nearest the 'toe' of the weld are shown in Fig. 14. The stress approaches 300 MPa, the yield strength of the steel, and is well in excess of the design stress of 140 MPa. It was concluded that 1 kg is the largest charge mass that can be deontated without exceeding the static yield stress of the vessel.

Calculation of the strain rate indicates values of approximately 2 s^{-1}, and using this value in the Cowper Symonds equation for strain rate effects, $\sigma_y/\sigma_0 = 1 + \dot{\epsilon}_0/D)^1/p$ where σ_y is the yield strength, σ_0 is the static yield strength and D and p are material constants, (for mild steel p = 5 and D = 40) indicates an increase in the yield strength of about 50%.

Thus even allowing for strain rate effects in the design stress of a 50% increase 1 kg of explosive is too close to the safe limit of this chamber. In practice a generous safety margin has to be allowed.

However, 1 kg charge gives a first peak strain of 2.5×10^{-4}. This is five times that of the one produced experimentally and theoretically by the 106 g charge. The linear relation between the charge mass and the peak pressure (which is proportional to the strain) at low values is not valid at higher charge masses. Larger charge masses produce relatively lower peak strains and consequently lower peak stresses. Further experimentation will be needed for more accurate definitions of the non-linear relationship. In the meantime, the charge limit is set to 300 g. A full analysis of the vessel needs to be carried out at this charge mass.

Results of Short Analyses of Several Charge Masses

Due to lack of computer and data interpretation time it has not been possible to undertake full analyses of other charge masses. However, the magnitude of the first peak strain has been obtained for eight other charge masses extending the range to 15-1000 g. The results are plotted, with the experimental data, in Figure 15. The experimental data are less than the predicted values for low charge masses, but asymptotically approach the predictions near to 60g. The reasons for this discrepancy, with experimental data values only 70% of predicted cannot be determined without further investigation, but it is probable that incomplete detonation of the very small (less than 2cm radius) charges is responsible. This hypothesis could be checked by using a plastic explosive charge of similar yield. A datum at about 300g of explosive would be helpful.

CONCLUSIONS

Experiments using small charges have been performed and have validated both closed form and numerical analyses.

A literature review showed that the phenomenon of 'swinging' whereby large deformations evolve after several cycles was well known and documented. The numerical analysis correctly predicted this, but the closed form analyses was not capable of extension.

The numerical analysis also showed that the vibration modes of the nozzles were important and tended to become the predominant oscillation.

The design limit was found by (i) extending experimental data fitted to a closed form analysis leading to a safe limit of 1.5 kg and (ii) finite element analyses concentrating on the stress raising properties of the sphere nozzle junction, leading to a safe limit of 1 kg.

Both theory and experiment indicated that the strain rate, at about $2 \ s^{-1}$, was high enough for strain rate strengthening effects to take place, thus increasing safety margins.

FUTURE WORK

The work has shown that FE is invaluable in extending confident safe limits of real structures. Future work will involve a further modelling of the process to ensure that no major quantitative effects are ignored by the simple axisymmetric half model used. The analysis has been on stress-free models. A full plastic analysis, at say 2 kg of explosive, will indicate the extent of plastic deformation, and may indicate that shakedown effects will be beneficial.

The effect of non-central charges will be investigated with the aid of strain gauges and pressure transducers at critical points within the vessel.

SYMBOLS USED

Note: The original notation has been retained in the literature review.

a_0 = speed of sound in air (340.29 ms^{-1})

a = internal radius of vessel (m)

b = external radius of vessel (m)

E = Young's modulus (Nm^{-2}), total energy of blast source (J)

h = shell thickness (m)

I = impulse per unit area (Nsm^{-2})

m = Mach number

P = pressure (Nm^{-2})

P_O = atmospheric pressure (10^5 Nm^{-2})

P_p = peak blast overpressure (Nm^{-2})

R = distance from blast source (m)

T = blast overpressure duratin (s)

u_r = radial displacement (m)

W = explosive charge mass (g)

β = parameter in modified Friedlander equation

ϵ = strain

σ = stress (Nm^{-2})

ω = radial frequency of oscillation ($rads^{-1}$)

REFERENCES

1   Baker W E and Allen F J, "The Response of Elastic Spherical Shells to Spherically Symmetric Internal Blast Loading", Proc. 3rd US Nat Congress Appl Mech, p 79-87, New York, 1958.

2   Baker W E, "The Elastic-Plastic Response of Thin Spherical Shells to Internal Blast Loading", Ballistic Research Laboratories, Aberdeen Proving Ground, Mem ASME J of Appl Mech, p 139-144, March 1960.

3   Zhdan S A, "Dynamic Load Acting on the Wall of an Explosion Chamber", Combustion, Explosion and Shock Waves, Vol 17, No 2, p 141-144, 1981.

4   Buzukov A A, "Characteristics of the Behaviour of the Walls of Explosion Chambers Under the Action of Pulsed Loading", Combustion, Explosion and Shock Waves, Vol 12, No 4, p 549-554, 1976.

5   Buzukov A V, "Forces Produced by an Explosion in an Air-Filled Explosion Chamber", Combustion, Explosion and Shock Waves, Vol 16, No 5, p 555-559, 1980.

6   Vasil'ev A A and Zhdan S A, "Shock-Wave Parameters on Explosion of a Cylindrical Charge in Air", Combustion, Explosion and Shock Waves, Vol 17, No 6, p 669-673, 1981.

7   Adishchev V V And Kornev V M, "Calculation of the Shell of Explosion Chambers", Combustion, Explosion and Shock Waves, Vol 15, No 6, p 780-784, 1979.

8   Kornev V M, Adishcev V V, Mitrofavov A N and Grekhov V A, "Experimental Investigation and Analysis of the Vibrations of the Shell of an Explosion Chamber", Combustion, Explosion and Shock Waves, Vol 15, No 6, p 821-824, 1979.

9   Ivanov A G, Ryzhanskii V A, Tsypkin V I and Shitov A T, "Scale Effect in the Strength of a Pressure Vessel Under Internal Explosive Loading", Combustion, Explosion and Shock Waves, Vol 17, No 3, p 327-330, 1980.

10 Ivanov A G, Novikov S A and Sinitsyn V A, Fiz Geroniya Vzryva, 8, No 1, (1972) Dokl Akad Nauk SSSR 194, 1970

11 Ivanov A G And Mineev V N, Dokl Akad Nauk SSSR, 220, 1975

12 Ivanov A G And Mineev V N, Fiz. Geroniya Vzryva, 15, No 5, 1979.

13 Ahrens J T, Allen F C and Kovach L R, "Explosive Gas Blast: The Expansion of Detonation Products in Vacuum", J of Appl Phys, Vol 42, No 2, p 815-829, 1971.

14 Lutzky M, Naval Ordnance Laboratory, NOL-TR-62-19, 1962.

15 Dawson P H and Alexander K, "An Enclosure for Explosive Processes", Proc of 7th Int Conf on High Energy Rate Fabrication, Leeds, p 39-47, 1981.

16 Gill S S, Kitching R, Kannas A and Paine R T, "Experiments on Spherical Pressure Vessels with Pad-Reinforced Nozzles", Chapter 3, Applied Mechanics Division, UMIST, UK.

17 Paine R T, MSc Thesis, University of Manchester, 1976.

18 Kannas A, MSc Thesis, University of Manchester, 1975.

19 Baker W E, "Explosions in Air", University of Texas Press, 1974.

20 Baker W E, Cox P A, Westine P S, Kulesz J J, Strehlow R A, "Explosion Hazards and Evaluation", Elsevier Scientific Publishing Company, 1983.

sjb/km/chamber/9.1.91
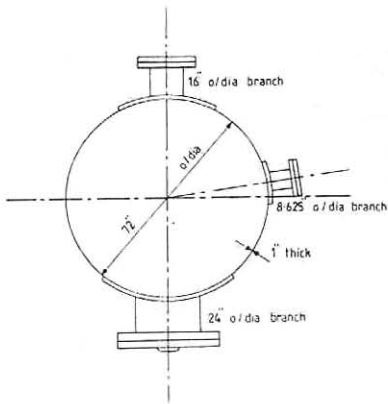
Figure 1 Explosive chamber under analysis (17)
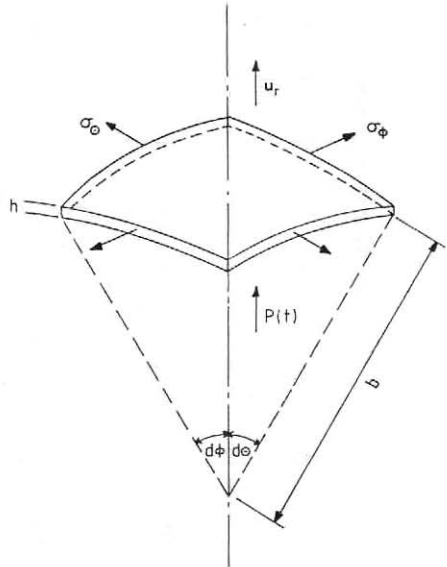
Figure 2 Element of a spherical shell under transient pressure

(a) 56 gms, pure Trimonite 1.

(b). 106 gms, pure Trimonite 1.
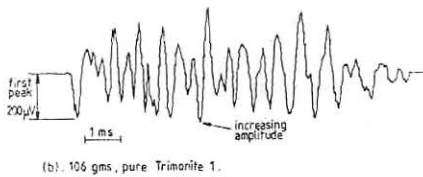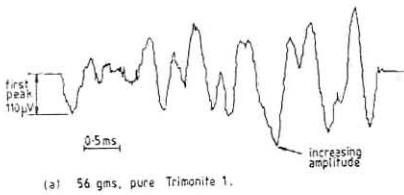
Figure 3 Typical oscillographs showing oscillations of spherical shell

W = 42 g

W = 63 g
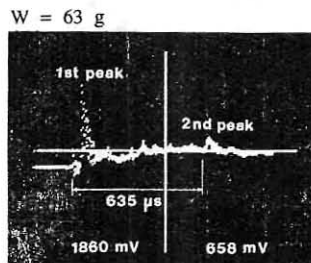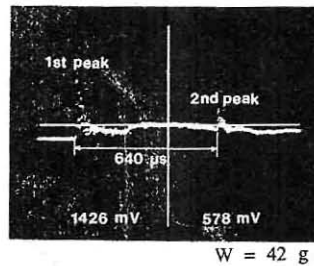
Figure 4 Typical pressure pulses (0.5 μs/sample, scale 2.5 V/MPa)
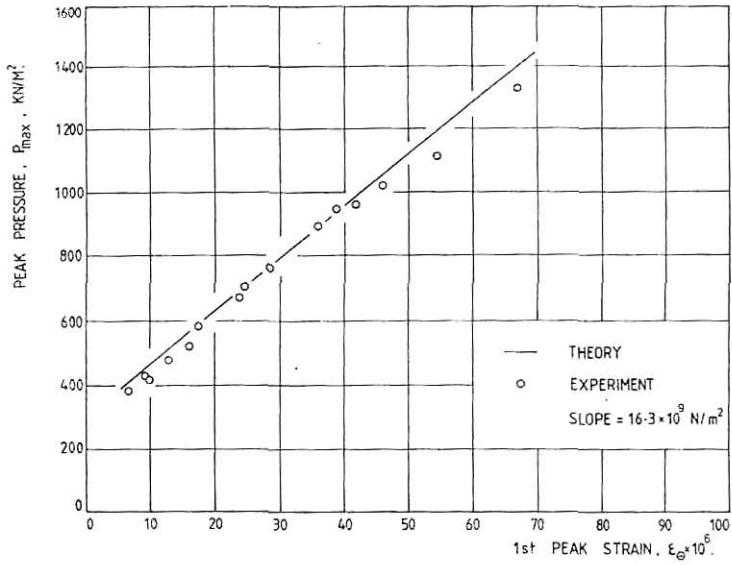
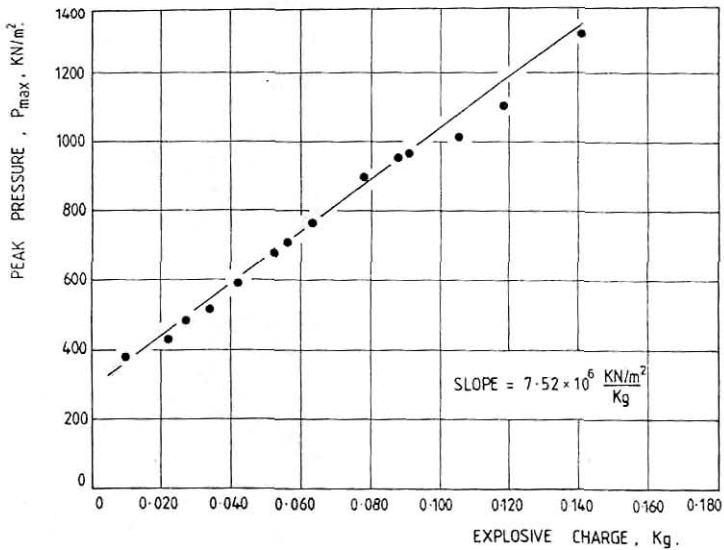Figure 5 Peak pressure versus hoop strain for various charges
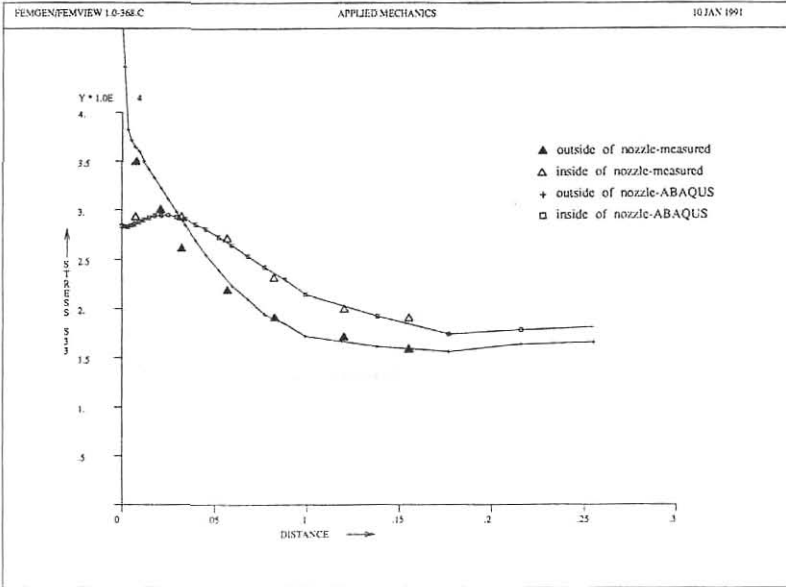

Figure 6 Peak pressure versus explosive charge

Figure 7a Experimental and finite element predictions of circumferential stresses along nozzle near sphere
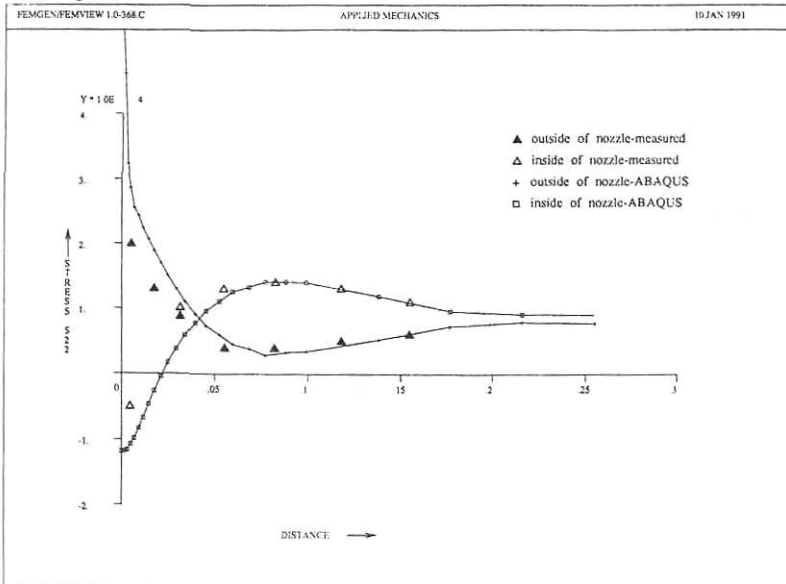
Figure 7b Experimental and finite element predictions of meridional stresses along nozzle near sphere
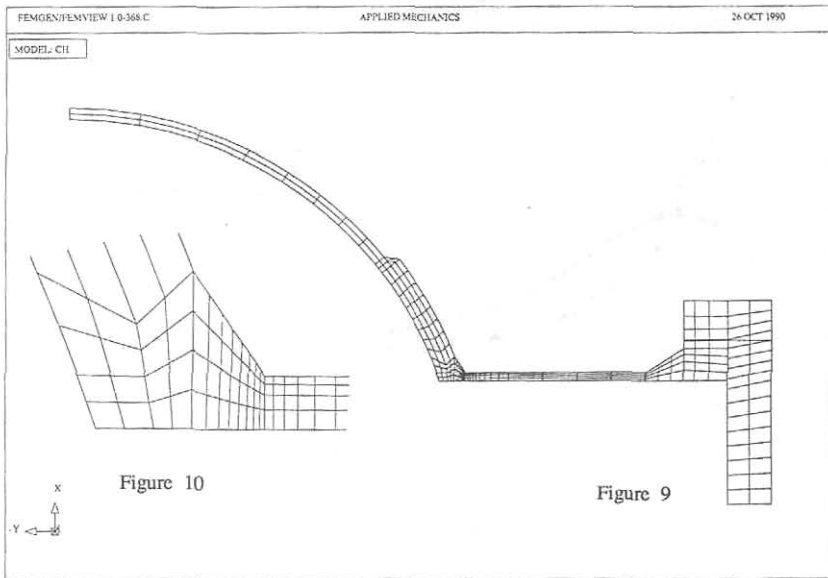
Figure 9 Finite element model and (inset Figure 10) detail of nozzle/sphere/pad weld
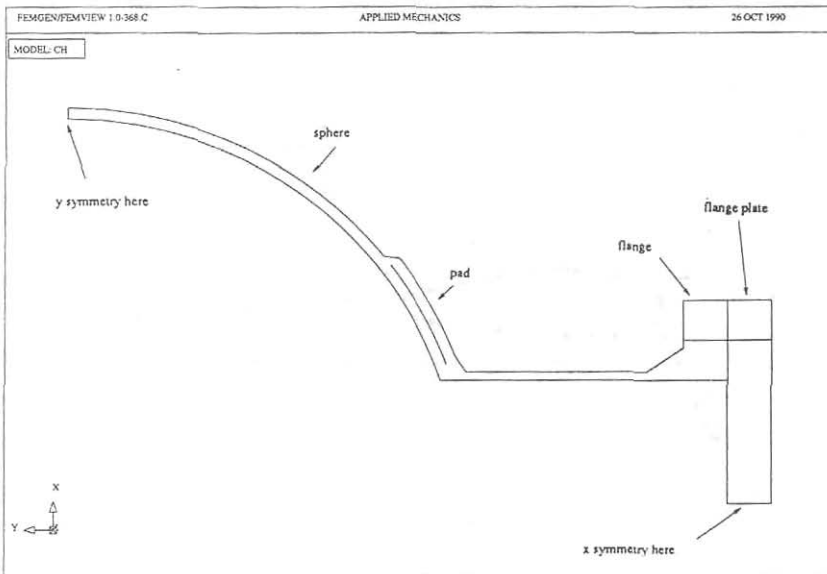
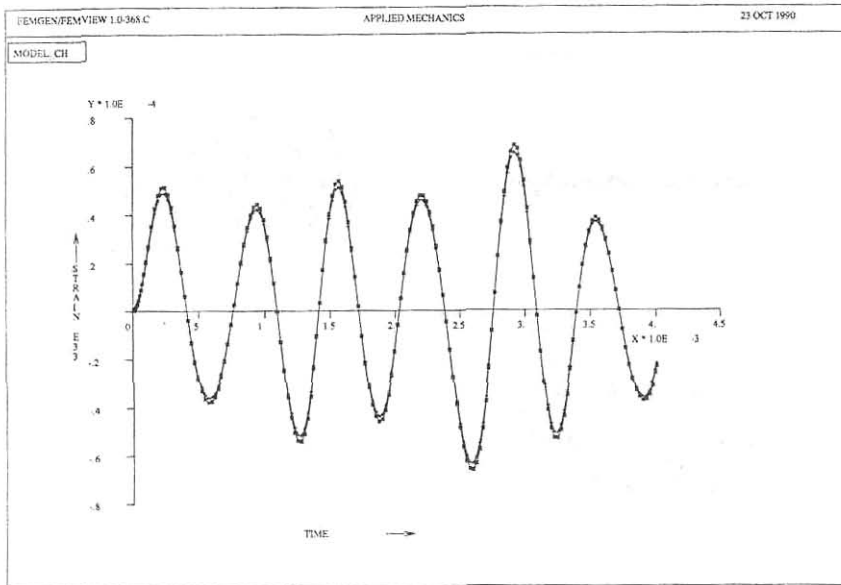Figure 8 Outline of finite element model for 0.61m diameter nozzle

Figure 11 ABAQUS prediction of hoop strain e33 versus time
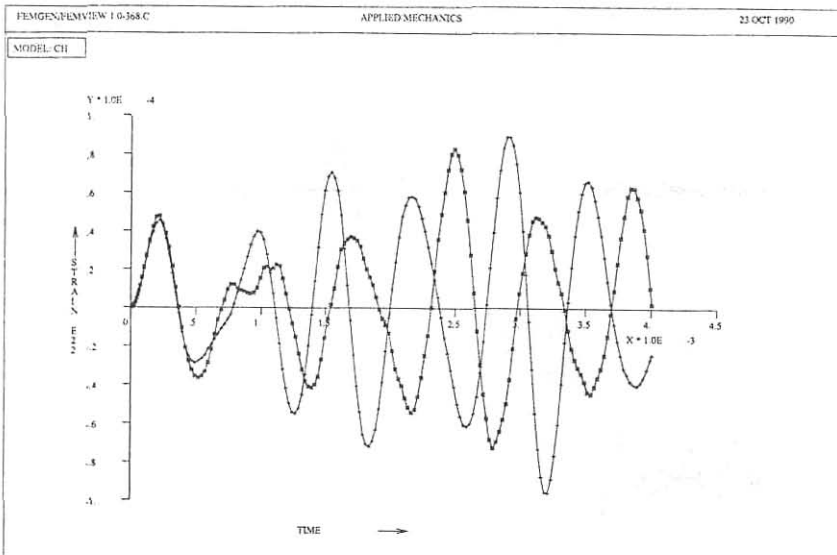
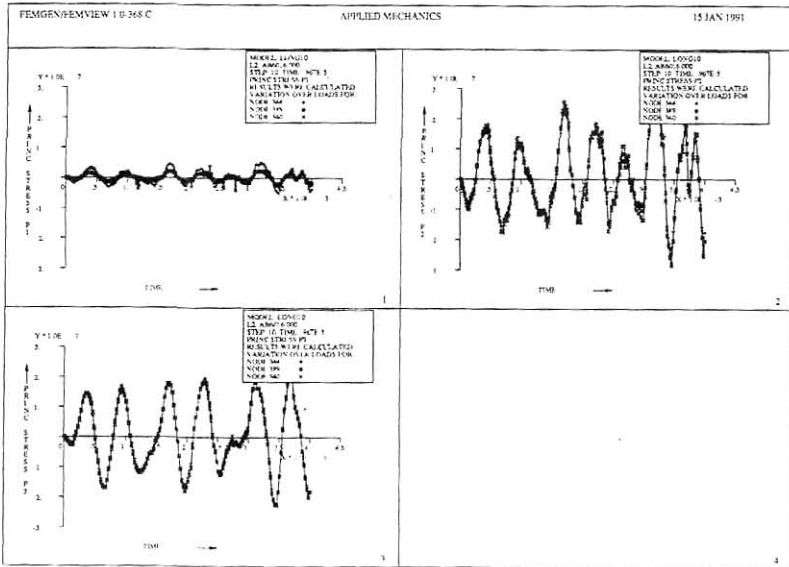Figure 12 ABAQUS prediction of meridional strain e22 versus time at inside and outside of vessel

Figure 13 ABAQUS prediction of principal stresses at three points nearest toe of weld for a charge mass of 106g
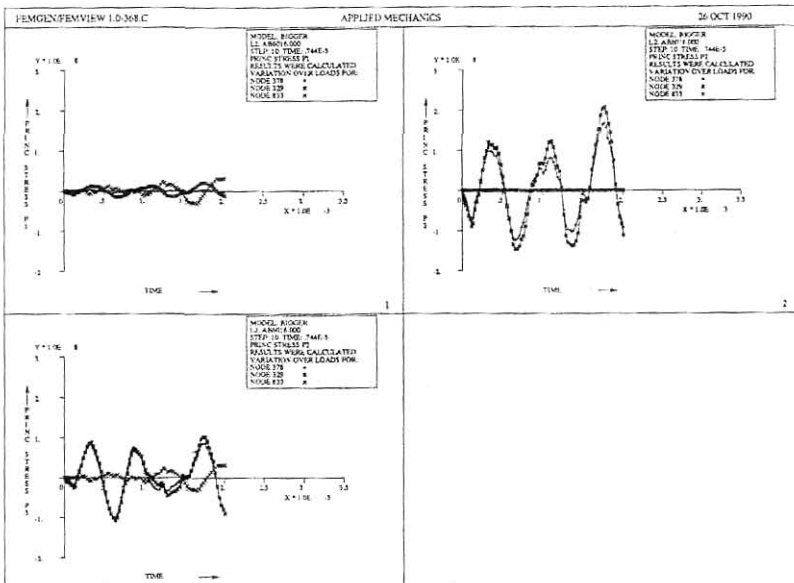

Figure 14 ABAQUS prediction of principal stresses at three points nearest toe weld for a charge mass of 1000g

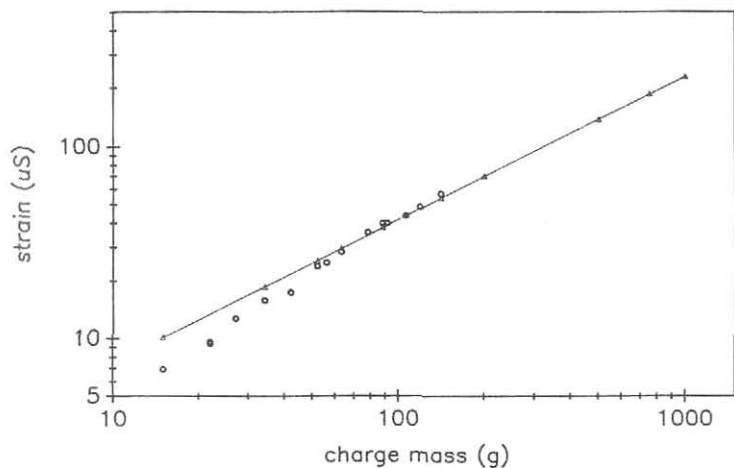o experimental data
▲ ABAQUS prediction e33

Figure 15 ABAQUS prediction of first peak strain and experimental data points